3ACTION: A VIABLE SETUP FOR DIRECT-TENSILE TESTING OF CONCRETE

ROBERTO FELICETTI[*], RAMIN YARMOHAMMADIAN[*] AND E. CANTU[†]

[*] Politecnico di Milano, Piazza Leonardo da Vinci 32, 20133 Milan, Italy
e-mail: roberto.felicetti@polimi.it , ramin.yarmohammadian@polimi.it

[†] CONTROLS Group, Via Salvo d'Acquisto 2, Liscate, 20060 Milan, Italy
enrico.cantu@controls-group.com

Key words: direct tension test, cohesive fracture, test stability

Abstract: The experimental characterization of concrete's post-peak stress vs crack opening curve is a key aspect in many practical problems involving crack stability, like size-effect and explosive spalling of High-Performance concrete in the fire. The direct-tension test is recognized as the most straightforward solution, though the strain-softening material behaviour entails tricky issues concerning the axial and flexural stability of the test. Axial stability is impaired by the deformability of the loading frame since the traditional scheme of universal testing machines entails compression of rather long columns and bending of the crosshead and the table. The consequent deformation energy largely exceeds the dissipation capacity of the tested sample, requiring responsive closed-loop control systems for smoothly driving the descending branch of the test. As regards flexural stability, several solutions have been proposed to improve the bending stiffness of the test rig, mostly based on ball bushing guiding systems or adjustable tie-rods secured to the loading platens. However, the transversal restraint to the sample may trigger parasitic shear stress, which translates into inclined fracture propagation paths and overlapping cracks.

To address these multifaced issues, an innovative frameless test rig has been designed, based on three symmetrically arranged electro-mechanical jacks directly pushing the top of the sample up. The samples are short, notched cylinders (Ø=100mm, h=150mm) preliminarily glued to thick steel platens and then bolted to the bottom table and the moving head of the machine, speeding up their installation and later removal. The load is exerted through stiff load cells and pendular struts, preventing any transversal load component. The actuators are optimized for stiffness and promptness, and three parallel control loops are implemented to drive the mean opening and two orthogonal rotation components of the crack mouth.

At the present stage, the prototype has been assembled and the control routines are being tested. A first series of experimental results will be included in the final presentation at the conference.

1 INTRODUCTION

The observed behaviour of concrete in tension depends to a large extent on the experimental tools that are used. The most common test methods are the direct-tension test, the splitting (Brazilian) test and the bending tests (e.g. three-point bending), with the increasing impact of structural effects due to the inhomogeneous stress distribution across the fracture plane (Figure 1) [1]. Then, the derived tensile parameters are different [1–3] and direct tension is generally preferable since it provides more objective values of tensile strength and fracture energy, with no need to rely on reverse interpretation techniques [5–8]. On the other hand, implementing a direct tensile test is quite challenging because of several technical issues.
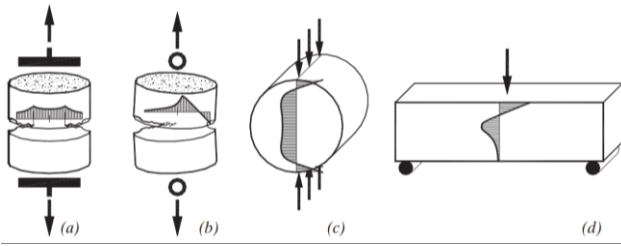
Figure 1: Outlines the stress patterns in the usual tensile tests: direct tension with (a) restrained and (b) hinged ends; (c) splitting test and (d) bending test [1]

The softening behaviour of quasi-brittle materials like concrete and rock entails a reduction of the borne load at increasing crack opening (namely a negative stiffness), requiring a displacement-controlled test system to drive the test [7–9]. Nonetheless, the smooth propagation of the crack at increasing actuator displacement would imply the total stiffness of the loading frame to be larger than the negative stiffness of the fracturing sample [10,11]. In actual fact, the typical slope of softening in ordinary and high-performance concrete (100-200MPa/mm [1]) and the common size of the fractured section ($\approx 10^4$ mm^2) lead to a MN/mm magnitude, which is tenfold larger than the frame stiffness of the available test rigs. Hence, a snap-back instability arises in the post-peak stage [12], and a responsive strain-driven closed-loop control system is then required.

Another consequence of the negative stiffness in the material response is the tendency of the sample to bend, due to a kind of reverse buckling [13]. As a consequence, the fracture starts propagating from the weakest side of the sample, leading to a remarkably not uniform stress pattern (see Figure 1-b).

Different passive solutions have been proposed to improve the flexural stiffness of the test rig, based on ball bushing guiding systems [14] or adjustable tie rods secured to the loading platens (**Figure 2**, [14])
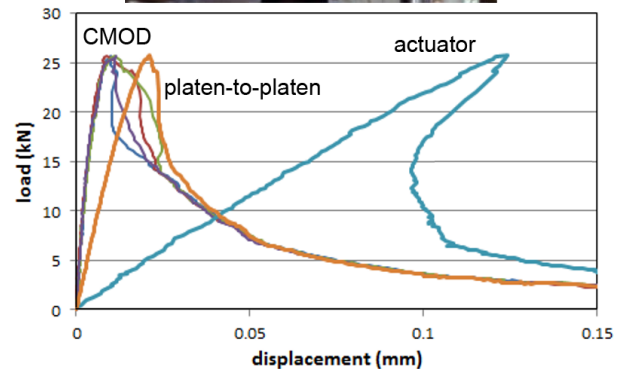

Figure 2: Modified electro-mechanical Instron testing machine retrofitted with adjustable tie-rods to enhance the flexural stiffness, residual CMOD scatter and snap-back due to the deformability of the frame [14]

In one case, two additional actuators were used to actively control the uniformity of the crack opening [15]. However, some concerns arise regarding the possible shear stress developing in these redundant restraint systems. The consequent rotation of the principal stress direction may lead to inclined crack propagation paths and twin overlapping fractures, with a milder softening response and an overestimation of the dissipation capacity of the material [16].

To address these fundamental issues, an innovative frameless setup was developed aimed at converting this advanced research experiment into a routine laboratory test. The original concept and the technical solution developed in this project are discussed in the following sections.

2

2 CONCEPT OF THE TEST SETUP

One first cornerstone to be reassessed is the rational behind the traditional universal test frame. In that scheme, pulling a sample entails compressing rather long columns and bending the machine table and crosshead, with a significant elastic deformation (typical frame stiffness around 200kN/mm). Moreover, securing both ends of the specimen to not bendable press platens is quite difficult, due to the very tight tolerances. In many cases, the sample is directly glued to the platens, with a remarkable impact on viability.

To solve these problems, a compact tabletop solution was devised, where three actuators symmetrically arranged around the sample directly push the top of the sample up through a removable crosshead (Figure 3).
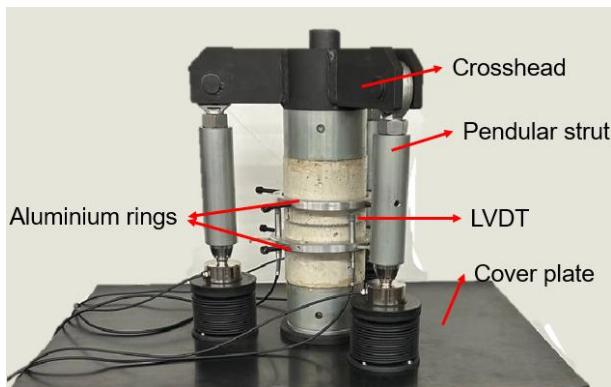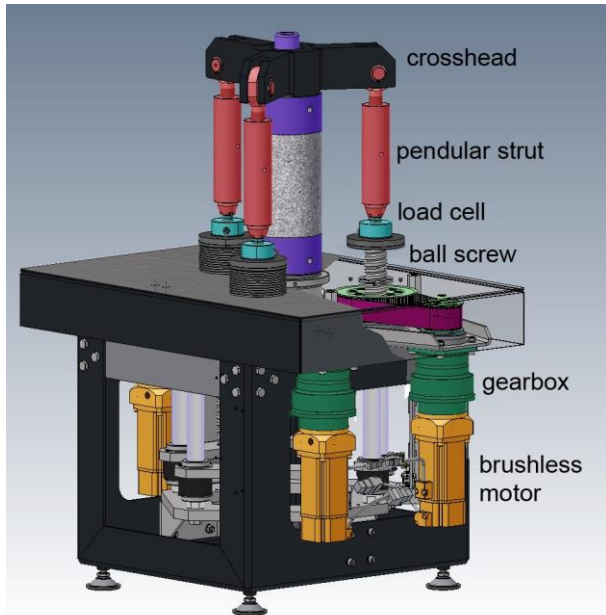
The rotating nuts are actuated by low-inertia brushless motors, through precision gearboxes and a toothed belt transmission. In this scheme, the sample is separately glued to thick steel blocks and then screwed to the baseplate. Then, the crosshead is bolted to the top of the specimen and the hinged pendular struts are aligned with the load cells to instate the initial contact.

The actuators are electromechanical jacks, which allow higher stiffness and better accuracy than the hydraulic solution (being not affected by the compressibility of oil). Ball screws with rotating nuts were adopted to minimize the length of the loaded shaft. This requires providing the shaft with an anti-rotation unit (Figure 4) but also minimizes the torsional disturbance induced by the load cells.
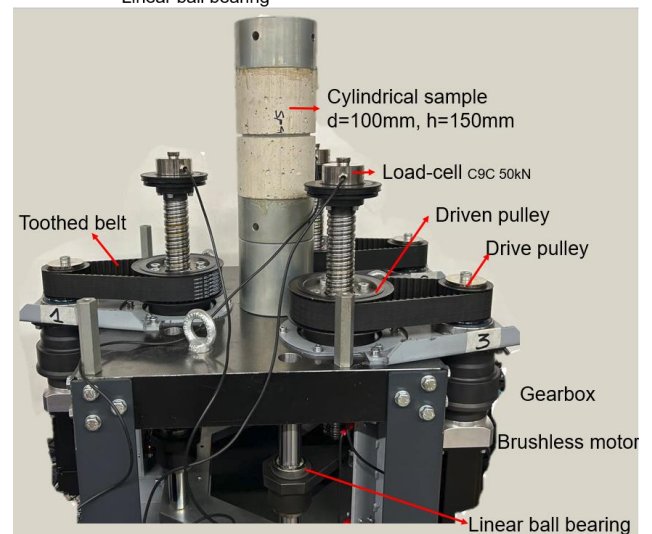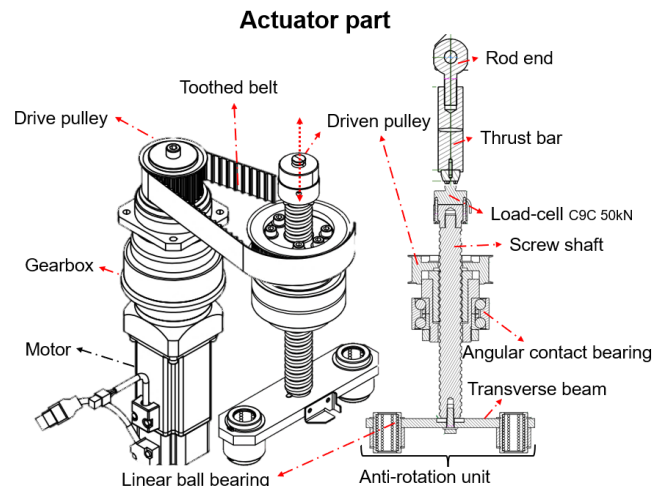

Figure 3: General scheme of the new setup and components of the electromechanical transmission.

Figure 4: Details of one actuator, including the bearings and the anti-rotation unit.

Concerning the sample geometry, 100mm diameter notched cylinders were preferred (notch depth 9mm, sample length 150mm). As experienced in former research projects [1,17], radial symmetry promotes the propagation of a single planar crack, as would be possible in prismatic samples just with the introduction of lateral guide notches [14]. The length ensues from the opposite requirements to allow a smooth stress diffusion from the glued edges while minimizing the axial deformability of the sample. Though moulded cylinders generally imply testing parallel to the casting direction (with the possible influence of bleeding below the coarse aggregates in low-grade mixes), the option of drilling cores from standard cubes or existing structures is also available.

3 TECHNICAL ASPECTS

Direct tensile testing of concrete entails very tight requirements as concerns the stiffness of the test rig and the sensitivity and promptness of the data acquisition system. As a reference, both the elastic stiffness and the negative slope of the softening branch are in the range of 1-2MN/mm and the Crack Opening Displacement at the load peak is about 20microns. These figures informed the design of the different components of the setup.

3.1 Mechanical design

The starting point in the design process was the definition of the actuator's full scale (about 30kN each) and the thickness of the solid steel baseplate accommodating them (plate thickness = 58mm, stiffness ≈3MN/mm). Also, the angular contact ball bearings (120x20mm, rated static load 156kN) and the ball screw (32x10mm, rated static load = 83kN) were oversized, to the advantage of the overall stiffness. The same objective informed the selection of the load cells (HBM C9C, 50kN full scale, 670kN/mm stiffness), the drive belt and the spherical rod ends (SKF SA20ES, rated static load 42kN) of the pendular struts.

To be mentioned is that in the case of three parallel actuators exerting a load on the sample, their axial stiffness sums up. Further investigations are in progress to check the impact of each component on the rig deformability and then on the stability of the test.

3.2 Electromechanical actuation

One pivotal aspect governing the actuator's ability to quickly implement small corrections to the applied displacement is the peak acceleration allowed by the motor and the transmission component. Low inertia 400W brushless motors have been selected for this application (Delta ECMA-CΔ0604-S, peak torque 3.8N.m, moment of inertia 18 kg.mm^2). Precise epicycloidal gearboxes were fitted to the motors (Neugart PSN90, 2 stages, 1:25 ratio, moment of inertia 16kg.mm^2, backlash < 1arcmin). A further 1:2 reduction was implemented with the toothed wheels of the belt transmission. The nominal peak acceleration (10^5rad/s^2, equivalent to 3.5m/s^2 at the actuator shaft) would allow to implement a 1μm displacement correction in less than 1ms ($\Delta u = \frac{1}{2} a_{peak} . \Delta t^2$) despite the very low velocity ($v = a_{peak} . \Delta t = $ a few mm/s) the motors are also fitted with 17bits magnetic encoders (130000 steps/turn) and are driven by accurate AC drives (Delta ASDA-A2) for close loop positioning.

3.3 Data logging

A responsive control system requires fast data acquisition with high resolution and low noise. A modular data logger has been selected based on separated amplifiers and analogue-to-digital converters connected via a RS485 bus (Orbit 3 by Solartron). The crack mouth opening displacement is monitored by 3 LVDTs (2mm range) controlling the distance between two aluminium rings secured via radial screws (initial gauge length 50mm, Figure 3). The 3 load cells have been connected to as many bridge amplifier modules. The communication is managed by an ethernet interface allowing fast data transfer to a PC (> 1000 data sets/s) and galvanic insulation of the analogue signals. In the first checks, the standard deviation of the

measuring channels under constant input were 0.1μm and 0.5N respectively. A further component of the system is a microcontroller (Teensy 4.0) monitoring the motor encoders (via optoisolators) and driving a multi-channel digital-to-analogue converter (Texas Instruments DAC81404) via a fast SPI serial port. In the first implementation of the control system, the outputs of the DAC will govern the velocity of the motors through the AC driver. As an alternative, trains of digital pulses may pilot the rotation of the motor shafts.

3.4 Control strategy

The control of three interconnected actuators entails the problem of their possible mutual interference, which may translate to the loss of accuracy and resonance. For this reason, the three CMOD measurements are combined to work out the mean crack opening and two orthogonal components of the rotation. Three independent control algorithms are then implemented (PID - proportional, integral and derivative) to impose a constant strain rate and a nil value of rotations. As an option, the combination with the load values could be considered to simulate the effect of a virtual bending stiffness, reproducing any boundary condition between fully hinged and fully restrained extremities.

In the prototype development stage, the control algorithm has been implemented in the LabVIEW environment and runs on a laptop. A future option is to assign the control loop to the Teensy microcontroller while keeping the PC as a user interface.

3.2 Concrete mixes and specimen preparation

Cylindrical concrete samples with and without polypropylene fibre were cast and cured in moist conditions for more than 6 months. Then, cylinders were cut and ground on both sides to have 150mm height and a notch was cut in the middle of the sample (9mm depth and 4mm thick). Just one day before the test, samples were glued to the top

and bottom of thick steel blocks (UHU plus Endfest 300 epoxy glue).

The interest in comparing plain and PP fibre-reinforced concrete is to prove a further working mechanism of this polymeric fibre in mitigating the risk of explosive spalling in fire. As is well known, the dispersed network of microcracks and voids generated by the thermal dilation and following melting of the filaments promotes the easier flow of vapour in hot concrete, reducing pore pressure and fostering material drying. Nonetheless, a possible side effect is also the reduction of the slope of the softening branch, and then of the material brittleness, as already observed in thermally damaged concrete [1]. Then, residual tests after a thermal cycle up to 200°C will be performed on both types of concrete to corroborate this concept.

Table 1: concrete mix

	without fibre	1.5 kg/m^3 PP fibre
Cement CEM III	400	400
Filler	280	368
Sand 0-4 mm	920	870
Gravel 4-10 mm	630	600
Effective water	160	160
w/c	0.4	0.4
Max aggregate size	10	10
Plasticizer (%cement weight)	2.2%	4.2%
Age at testing [day]	180	180

concrete strength class= C80

4   CONCLUSIONS

In this paper, a novel and viable setup has been presented aimed at performing fully controlled direct tension tests on notched concrete samples. Due to the demanding construction of the machine prototype and the pressing deadline for paper submission, no experimental results are presented yet. Nonetheless, the following conclusions can be drawn based on the finalized steps of the project.

The removal of the loading frame and the partition of the applied load among three parallel actuators are the key aspects of the proposed scheme. The adoption of a removable crosshead remarkably simplifies the

installation of the sample by bolting preliminarily glued steel blocks.

High stiffness of the test rig and promptness of the actuator control are the available tools to increase the chance of performing smooth and stable tests even in brittle fine-grained cementitious composites. Both directions have been taken in the design of the proposed setup, to maximize its working range.

Different disciplines of Engineering were involved in the design of the proposed test rig, from the definition of the structural layout to the choice of the mechanical components, from the architecture of the data logging system to the multi-axis control of electric motors. Nonetheless, the starting point was a clear view of the strict requirements and the open challenges entailed by fracture testing of brittle materials.

REFERENCES

[1] P. Bamonte, R. Felicetti, High-temperature behaviour of concrete in tension, Struct. Eng. Int. J. Int. Assoc. Bridg. Struct. Eng. 22 (2012) 493–499.

[2] S.J. Choi, K.H. Yang, J. Il Sim, B.J. Choi, Direct tensile strength of lightweight concrete with different specimen depths and aggregate sizes, Constr. Build. Mater. 63 (2014).

[3] S. Swaddiwudhipong, H.R. Lu, T.H. Wee, Direct tension test and tensile strain capacity of concrete at early age, Cem. Concr. Res. 33 (2003).

[4] T.H. Wee, H.R. Lu, S. Swaddiwudhipong, Tensile strain capacity of concrete under various states of stress, 52 (2015) 185–193.

[5] S. Wu, X. Chen, J. Zhou, Tensile strength of concrete under static and intermediate strain rates: Correlated results from different testing methods, Nucl. Eng. Des. 250 (2012) 173–183.

[6] G.P.A.G. van Zijl, V. Slowik, R.D. Toledo Filho, F.H. Wittmann, H. Mihashi, Comparative testing of crack formation in strain-hardening cement-based composites (SHCC), Mater. Struct. Constr. 49 (2016) 1175–1189.

[7] R.H. Evans, M.S. Marathe, Microcracking and stress-strain curves for concrete in tension, Matériaux Constr. 1 (1968) 61–64.

[8] P.-E. Petersson, Crack growth and development of fracture zones in plain concrete and similar materials, (1981).

[9] H. Schorn, T. Berger-Böcker, Test method for determining process zone position and fracture energy of concrete, Exp. Tech. 13 (1989) 29–33.

[10] R. Gettu, B. Mobasher, S. Carmona, D.C. Jansen, Testing of concrete under closed-loop control, Adv. Cem. Based Mater. 3 (1996) 54–71.

[11] S. Okubo, K. Kukui, Y. Nishimatsu, Control performance of servo-controlled testing machines in compression and creep tests, Int. J. Rock Mech. Min. Sci. Geomech. Abstr. 30 (1993) 247–255.

[12] W.R. Wawersik, C. Fairhurst, A study of brittle rock fracture in laboratory compression experiments, Int. J. Rock Mech. Min. Sci. Geomech. Abstr. 7 (1970) 561–575.

[13] B.Z. P., C. Luigi, Why Direct Tension Test Specimens Break Flexing to the Side, J. Struct. Eng. 119 (1993) 1101–1113.

[14] H. Akita, H. Koide, H. Mihashi, Specimen geometry in uniaxial tension test of concrete, Proc. Fram. Taylor \& Fr. London. (2007) 243–248.

[15] A. Carpinteri, G. Ferro, Size effects on tensile fracture properties: a unified explanation based on disorder and fractality of concrete microstructure, Mater. Struct. 27 (1994) 563–571.

[16] J.G.M. van Mier, M.R.A. van Vliet, Uniaxial tension test for the determination of fracture parameters of concrete: state of the art, Eng. Fract. Mech. 69 (2002) 235–247.

[17] R. Felicetti, P. Gambarova, M.P. Sora, G.A. Khoury, Mechanical behaviour of HPC and UHPC in direct tension at high temperature and after cooling, Fibre Reinf. Concr. BEFIB' 2000.